*Computational Mathematics and Modeling, Vol. 11, No. 4, 2000*

# OSCILLATION MODES IN SUPERSONIC FLOWS INTERACTING WITH OBSTACLES

**G. S. Roslyakov and Yu. N. Sadkov**

UDC 533.6

The article presents a numerical analysis of the modes that arise when underexpanded supersonic jets hit an obstacle. The calculations are carried out for different unrated values and different obstacle geometries. Comparison with results of physical experiments is reported.

In this article we continue the numerical analysis of some topics associated with the creation of oscillation modes when an unrated supersonic jet hits an obstacle (see [1–3]). This subject has been considered by many authors during the last decade [4–10]. For applications it is relevant to consider a wide range of situations with various incident flow characteristics and various barrier geometries. In some cases, these oscillations are undesirable; in other cases, we strive to maximize them (as in the Hartman resonator). The mechanism of mode evolution in various cases is probably driven by common regularities. The study of these regularities as a function of controllable external conditions is a relevant topic. Difficulties arise due to the complex structure of the space-time interactions of different parts of the stream, multiplicity of factors influencing the result, and the need to track the dynamics of their behavior in a sufficiently large region adjoining the nozzle and the obstacle. Numerical methods are quite promising for the study of such complex processes, because computer experiments, as distinct from physical experiments, allow easy placement of sensors in all parts of the region and controllable variation of all relevant parameters.

We consider an axisymmetric model based on the Euler divergence equations in cylindrical coordinates $x$, $r$:

$$L(U) = \frac{\partial U}{\partial t} + \frac{\partial F(U)}{\partial x} + \frac{\partial G(U)}{\partial r} + H(U) = 0, \tag{1}$$

where

$$U = \begin{pmatrix} \rho \\ \rho u \\ \rho v \\ e \end{pmatrix}, \quad F = \begin{pmatrix} \rho u \\ p + \rho u^2 \\ \rho uv \\ (p+e)u \end{pmatrix}, \quad G = \begin{pmatrix} \rho v \\ \rho uv \\ p + \rho v^2 \\ (p+e)v \end{pmatrix}, \quad H = \frac{1}{r}\begin{pmatrix} \rho v \\ \rho uv \\ \rho v^2 \\ (p+e)v \end{pmatrix},$$

$u$, $v$ are the velocity components along the axes $x$, $r$, $p$ and $\rho$ are pressure and density, $e = 0.5\rho(u^2 + v^2) + p/(\gamma - 1)$ is the total energy, $\gamma$ is the adiabatic exponent.

The problem is stated in the following common form for all calculations. Initially, the entire numerical region $(0 < x < x_N,\ 0 < r < r_N)$ is filled with a stationary gas with the parameters $p_0$, $\rho_0$, $u = v = 0$, $\gamma$. The nozzle outlet section of radius $r_1$ is located at the left boundary $(x = 0)$, where the parameters of the injected homogeneous flow are defined as $u = u_1$, $v = 0$, $p = p_1$, $\rho = \rho_1$. Alternatively the flow parameters can be defined by specifying the Mach number $M_1$, the adiabatic exponent $\gamma$, and the unrated value $n$ for equal temperatures $T_0 = T_1$. At a distance $l$ from the nozzle there is an infinitely long cylindrical obstacle of radius $r_c$ (coaxial with the nozzle). The obstacle is a half-closed cavity with thin walls and depth $L$ whose open end faces the nozzle. In particular, for $L = 0$, this is a cylindrical plug. For large $L$, when the bottom part of the cavity extends outside the right boundary of the main numerical region $(x = x_N)$, one-dimensional equations are applied in this part of the cavity. In all alternatives, $\gamma = 1.4$. The following boundary conditions are specified: impermeable conditions for $x = 0$, $r > r_1$, on

Translated from Prikladnaya Matematika i Informatika, No. 3, pp. 71–80, 1999.

 1046-283X/00/1104-0382 $25.00 

the lateral walls and on the bottom of the cavity; so-called nonreflecting boundary conditions [11] on the remaining (free) boundaries, i.e., $r = r_N$, $0 < x < x_N$ and $x = x_N$, $r > r_c$. In some cases, when a negative radial velocity component $v < 0$ appeared, the pressure and density on the outer boundary $r = r_N$ were defined respectively as $\alpha p_N + (1-\alpha)p_0$, $\alpha\rho_N + (1-\alpha)\rho_0$, where $p_N$, $\rho_N$ are the values obtained from the nonreflecting conditions and $\alpha$ is variable. We used a third-order accurate explicit throughflow scheme [12] with increments $h_x = 0.1$, $h_r = 0.05$.

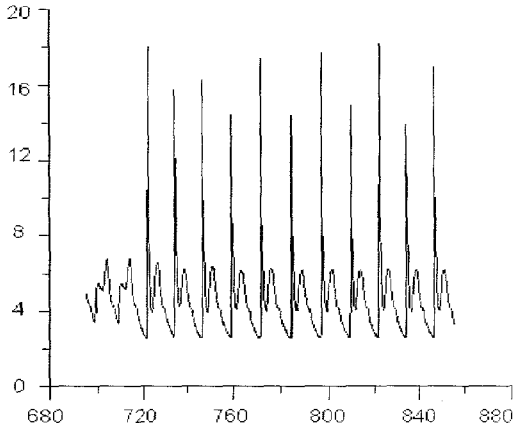


**Fig. 1**

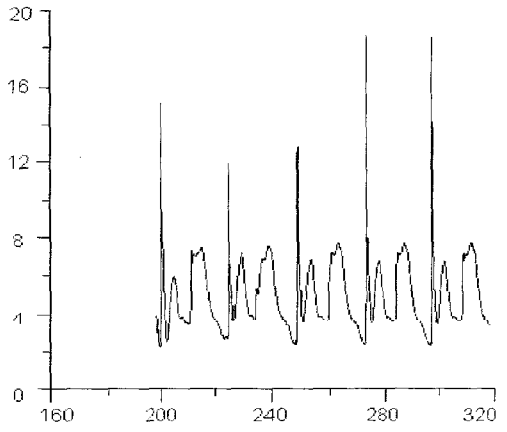


**Fig. 2**

We studied the incidence of supersonic jets with various Mach numbers $M_1$ and unrated values $n$ on obstacles of this type. The obstacle radius $r_c$, the cavity depth $L$, the distance from the nozzle to the obstacle $l$, and some of the boundary conditions were varied. The results are illustrated by graphs that plot the pressure oscillations at the bottom of the cavity and other points as a function of time $p(t)$. Changes of the unrated value $n$ lead to essential changes in the structure of the solution, and the results are accordingly presented separately for $n_1 = 1.2, 2, 3$.

**1.** With $n = 1.2$ the following initial values were specified: stationary gas parameters $\rho_0 = 1.8$, $p_0 = 1$; for supersonic flow from a nozzle of radius 1, $\rho_1 = 2.154$, $p_1 = 1.2$, $u_1 = 1.764$, $v_1 = 0$; radius of coaxial obstacle $r_c = 1$.

The flow structure and the evolution of oscillation modes for this case are described in detail in [1]. Here we present the numerical results that point to the dependence of the main parameters of these oscillations on the distance $l$ between the nozzle and the obstacle and the cavity depth $L$.

Figures 1–4 plot the variation of the period and the amplitude of pressure oscillations at the center of the plug

($L = 0$) with the distance $l$ taking the values 3.5, 4, 5.5, and 6, respectively. For $l = 3.5$ (Fig. 1) the oscillation period is $\approx 13$, although the alternation of bursts of larger and smaller amplitude shows that the value of $l$ is at the lower bound $X_H$ of the interval of $l$-values where lower frequency oscillations occur. Indeed, already for $l = 4$ (Fig. 2), the oscillation period is mainly $\approx 25-26$, although low-amplitude oscillations of higher frequencies are superimposed on this mode. The upper bound of this interval $X_K$ is for $l$ between 5.5 and 6 (Figs. 3 and 4). For $l \geq 6$ a high-frequency oscillation zone reappears.

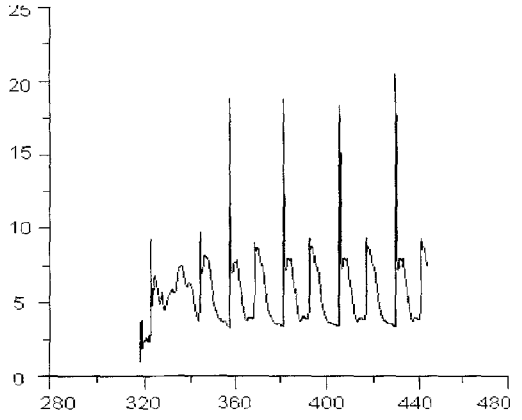


**Fig. 3**

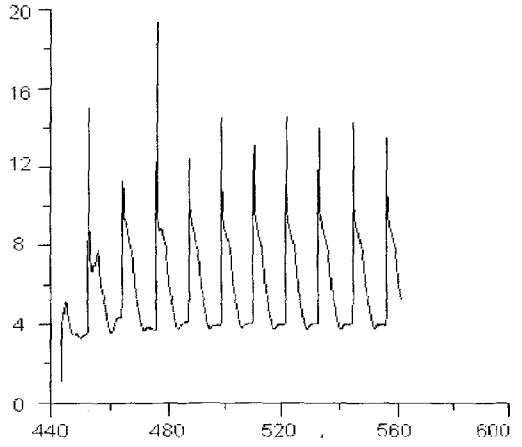


**Fig. 4**

Empirical formulas from [13] obtained from physical experiments with sufficiently long pipes give $X_H = (0.86M\sqrt{\gamma n} - 1)2 = 2.4$ for the beginning of the first zone of low-frequency oscillations and $X_K = (1.05M\sqrt{\gamma n} - 0.33)2 = 4.8$ for its end. Thus, with $L = 0$, this zone is displaced substantially, but its length does not change much and fits the experimental results.

Another series of calculations for $n = 1.2$ (Fig. 5) shows the dependence of the oscillations $p(t)$ on the geometry of the obstacle placed at distance $l = 4.5$ from the nozzle in the shape of a cylindrical cavity of depth $L = 4.5$ (broken curve) and $L = 8$ (solid curve). There is a good agreement in the oscillation period $D$ for a cavity with $L = 8$ as obtained from our calculations and from the formula of acoustic theory

$$D = \frac{4L}{c_0}. \tag{2}$$

We see from Fig. 5 that in the numerical solution $D \approx 38$, whereas formula (2) gives $D \approx 36.4$ for our case ($r_c = 1$, $p_0 = 1$, $\rho_0 = 1.8$).

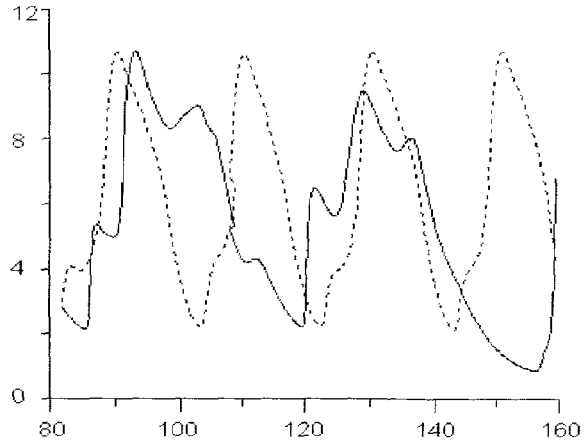


**Fig. 5**

**2.** For $n = 2$, the gas-dynamic and geometrical parameters correspond to those in [14]: $n_1 = 2$, $M = 1.5$, $r_c = 1.12 r_1$, $p_0 = \rho_0 = 1$, $\gamma = 1.4$, $u_0 = v_0 = 0$, $p_1 = \rho_1 = 2$, $u_1 = 1.7745$, $v_1 = 0$. In our calculations, $L$ and $l$ were varied. The physical experiments in [14] were carried out for a resonator with $L = 55.6$, $l = 8$.

The main qualitative difference in flow structure compared with $n = 1.2$ is the change in the impact of flows with a negative radial velocity component on the solution structure near the obstacle and their role in maintaining the oscillation modes. For $n = 1.2$ these flows and the cylindrical compression wave that they produce freely reach the axis in front of the obstacle, creating a zone of elevated pressure that has an essential impact on the evolution of oscillation modes. A resonance between two processes is observed. One of them is a shock wave along the axis between the jet and the waves reflected from the obstacle; the other is the previously mentioned radial flows that expand in a fan pattern from the axis when reflected from the obstacle (or blowing out from the cavity after reflection of compression waves from the bottom) and subsequently turn back toward the axis. Already for $n = 2$ the interaction of radial backflow with the peripheral part of the jet becomes more significant, raising the values of $p$ and $\rho$ at the edge of the obstacle compared with their values on the axis in front of the obstacle. This increases the flow intensity hitting the obstacle (or penetrating into the cavity) in the peripheral part and turns the incident flow along the plug in the direction of the axis (the same is observed inside the cavity) and generates axial backflow from the obstacle to the nozzle. For $n = 1.2$ practically no such flows were observed for $L = 0$, and the highest intensities in the flow hitting the obstacle and penetrating the cavity occurred near the axis; for $n_1 = 2$, on the other hand, high-intensity penetration into the cavity continues on the periphery even when the intensity of outflow on the axis is high. We report some specific data for this case with $L = l = 5$ (the pressure oscillations $p(t)$ at the center of the bottom are plotted in Fig. 6).

The initial penetration phase corresponds in Fig. 6 to point 1 ($t = 368$). For $r \approx 1$, $4.5 \le x \le 5$, i.e., near the mouth of the cavity, we observe negative $v$ values, $\min v \approx -0.2$, $\max p \approx 1.2$, whereas on the axis at the same distance from the cavity $\rho \approx 0.4$. In the mouth of the cavity $u \approx 0$ on the axis and $u \approx 1.2$ at the edge. In the pipe itself, $u < 0$ on the axis along the entire pipe length ($\min u \approx -0.5$).

In the next phase, the blow-in intensifies, especially at the edge, where $u > 0$ along the entire pipe length ($\max u \approx 1.2$), while on the axis $u < 0$ ($\min u \approx -0.4$). The stream begins to turn from the walls to the axis on the bottom of the cavity. In Fig. 6 this instant corresponds to point 2 ($t = 374$). Approximately at this instant, the cylindrical compression wave reaches the axis and the pressure is equalized before the entry into the cavity for $r = 0$ and $r = 1$. For $t = 376$ (point 3 in Fig. 6) these pressures become 3.3 and 2.3, respectively. We see from Fig. 6 that

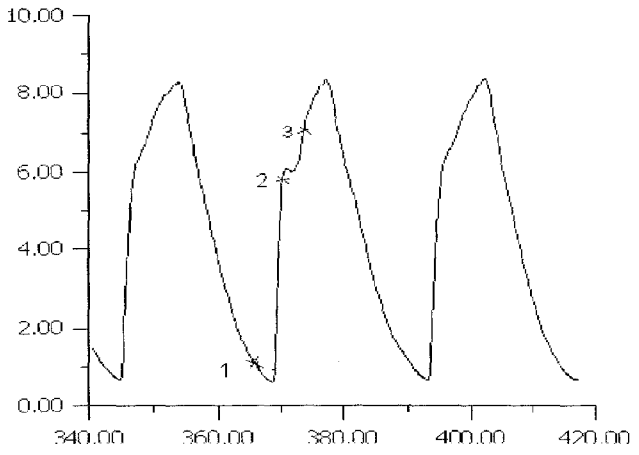


**Fig. 6**

at this instant $p(t) \approx 7$. Near the mouth of the cavity for $r = 1$ we have $\min v = -0.4$, $u \approx 1$, while on the axis $u < 0$ along the entire pipe length ($\min u = -0.4$). Subsequently, blow-out begins over the entire cross-section of the cavity mouth, but with much higher intensity on the axis. The negative $u$ zone extends along the axis much farther from the cavity in the direction of the nozzle than along the jet boundary, where the gas blowing out from the cavity collides with the jet and turns around, changing into a rapidly growing fan that spreads with supersonic velocity. The main numerical data characterizing the dynamics of the processes near the obstacle are presented in Table 1.

We now compare the calculations with the results of the physical experiment for $n = 2$, $L = 55.6 r_1$, $l = 8 r_1$ from [14], which gives the pressure oscillogram $p(t)$ on the bottom of the cavity in physical units. The following values can be extracted from the oscillogram: period $D \approx 0.009$ sec, oscillation amplitude $\Delta p = p_{\max} - p_{\min} \approx 8 \cdot 10^5$ Pa, dimensionless amplitude $\Delta p / p = 8$, since $p_0 = 1$ atm $\approx 10^5$ Pa. The period $D$ can be normalized by the nozzle radius $r_1$. We use formula (2). Substituting the dimensional period $D$, $c_0 = 30{,}000$ cm / sec, and $L = 55.6\, r_1$, we obtain $r_1 \approx 1.21$ cm. Given this $r_1$, we normalize the time $t$ dividing it by $r_1 / \sqrt{p_0 / \rho_0}$, and we obtain for the period $D \approx 188$ dimensionless units.

**Table 1**

| $t$ | $t_1 = 368$ | $t_2 = 374$ | $t_3 = 376$ |
|---|---|---|---|
| max ρ before entry into cavity for $r = 1$ | 1.2 | 2 | 2.3 |
| min ρ before entry into cavity for $r = 0$ | 0.4 | 2 | 3.3 |
| min $v$ before entry into cavity for $r = 1$ | −0.2 | −0.3 | −0.4 |
| $u$ inside the mouth of the cavity on the axis | 0.2 | 0 | −0.2 |
| $u$ inside the mouth of the cavity for $r = 1$ | 1.2 | 1.2 | 1 |
| ρ at the bottom of the cavity ($r = 0$) | 0.7 | 3.8 | 4.8 |
| ρ at the bottom of the cavity ($r = 1$) | 0.7 | 4.1 | 5.1 |
| $p$ at the bottom of the cavity ($r = 0$) | 0.09 | 6.0 | 7.0 |

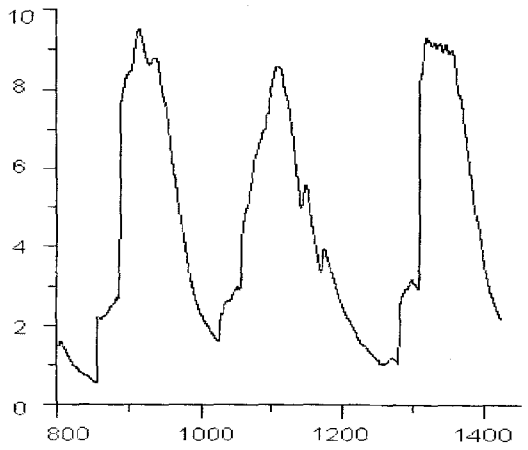


**Fig. 7**

Let us compare these experimental values of $\Delta p$, $D$ with the calculated values in the graph of $p(t)$ (Fig. 7) obtained on a grid with the same increments but in a numerical region with a larger radius $r_N = 10.5$. Calculations confirm that there is no need to enlarge the numerical region in the $x$ direction. In the pipe proper, starting at a distance 5 from its mouth, the calculations were carried out using the one-dimensional model.

Mode calculations with such a long period involve considerable computer time requirements, and tens of periods have to be computed to reach a steady periodic regime. It is therefore not surprising that the graph reveals considerable differences in the behavior of $p(t)$ in different periods. We accordingly average over the three periods shown in Fig. 7,

$$p_{\max} = \frac{(9.5 + 8.8 + 9.1)}{3} \approx 9.1, \qquad p_{\min} = \frac{(0.6 + 1.7 + 1.1)}{3} = 1.1,$$

whence $\Delta p = 8$. This matches the result obtained from the oscillogram. The average for $D$ is obtained as $1/3$ of the distance in $t$ between the extreme points $\min p$, i.e., approximately $(1430 - 850)/3 \approx 193$, or as half the distance between the extreme $\max p$, i.e., $0.5(1320 - 920) = 200$. In both cases, the values deviate by no more than 5% from the experimental result ($D = 188$).

The comparison thus justifies the proposed procedure for the study of low unrated supersonic jets flowing past obstacles.

**3.** With $n = 3$ we investigated the dependence of the flow past a cylindrical plug on its radius $r_c$ and on the boundary conditions. Initial values: $M_1 = 1.5$, $u_1 = 1$, $v_1 = 0$, $p_1 = 0.317$, $\rho_1 = 1$, $u_0 = v_0 = 0$, $p_0 = 1/3\, p_1 = 0.1056$, $\rho_0 = 1/3\, \rho_1 = 0.333$, $l = 6$.

The main qualitative changes compared with the cases $n = 1.2$ and $n = 2$ are associated with further increase in the role of the interaction of radial backflow with the peripheral part of the jet in forming the structure of the solution near the obstacle. For $n = 3$ the phenomenon of turning flow from the edge to the center of the plug and then along the $x$ axis from the plug to the nozzle is typically observed over a large part of the period, from the phase of high-intensity streaming of the jet to the plug associated with fanning out to the phase when gas flows away from the plug across the entire section ($u < 0$ for $r \le r_c$). During this entire time interval, a region with negative $u$ values is observed on the axis adjoining the plug.

The essential role of radial backflow for $n = 3$ is confirmed by calculations in which this backflow is blocked on the outer boundary $r = r_N$, specifically: instead of the $v$ value computed by the ordinary algorithm we take $\tilde{v} = 0.5(v + |v|)$. The graph in Fig. 8 includes this blocking from jet startup to $t = 40$, and oscillations virtually are not observed. Then for $t \in (40, 150)$ the blocking is removed, oscillations appear, and their amplitude rapidly increases. For $t > 150$ the blocking is again turned on and the oscillations are damped.

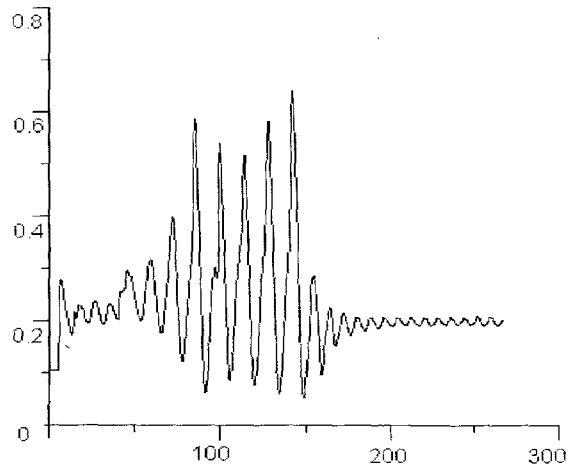


**Fig. 8**

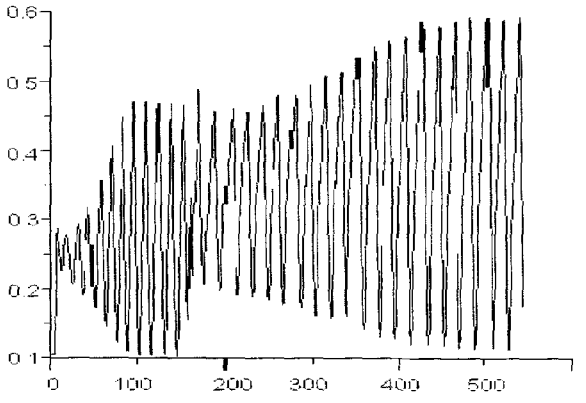


**Fig. 9**

The calculation results show, on the one hand, that the radial extent of the numerical region ($r_N = 3.5$) is insufficient and, on the other, confirm the fundamental possibility of influencing the oscillation modes through the peripheral region. As $r_N$ is doubled to 7, negative radial velocity components appear already inside the region, at a distance of 3–3.5 from the axis, and blocking produces the same results.

On the whole, the results of our numerical experiments demonstrate the substantial role of peripheral flow with a negative radial velocity component in the formation of oscillation modes. Their interaction with the jet is the most essential in the region between the central jump and the obstacle. This in fact is responsible for the transverse beating of the jet near the obstacle, which changes the proportion of energy of the supersonic part of the jet that goes into the interaction with the obstacle. As a result, we observe first a peripheral pressure maximum at the edge of the plug and then a compression wave propagating toward the axis. If this process unfolds synchronously with the arrival and reflection from the plug of a wave traveling along the axis from the central jump, the maximum pressure increase is achieved at the center of the plug. If there is a phase shift between the radial and axial processes, two local pressure maxima appear at the center of the plug. When the same jet hits a large-diameter plug, so that the entire jet interacts with the obstacle all the time, transverse oscillations of the jet do not produce this effect, and the oscillation amplitude determined primarily by axial shock processes decreases by a factor of several times. The maximum $p$ on the obstacle also drops sharply.

Another series of calculations deals with the effect that the blow-in of a subsidiary rated supersonic jet through a ring nozzle of radius $r_1'$ adjoining the central nozzle has on the amplitude of oscillation modes. Both $r_1'$ and $r_c$ were varied. The plot of $p(t)$ in Fig. 9 shows that the oscillation amplitude in principle can be increased by turning

on a subsidiary ring jet. Here a jet with previously specified parameters flows past a cylinder of radius $r_c = 1.7$ and no subsidiary blow-in occurs up to $t = 150$. Oscillation modes with a certain amplitude are established. Blow-in through a ring nozzle with external radius $r_1' = 1.5$, $M_1' = 1.5$ is turned on at $t = 150$. This perturbation breaks up the previously established steady state and produces a marked reduction of the amplitude; then a new steady state is established with oscillations of greater amplitude than before blow-in. The period $D$ also increases.

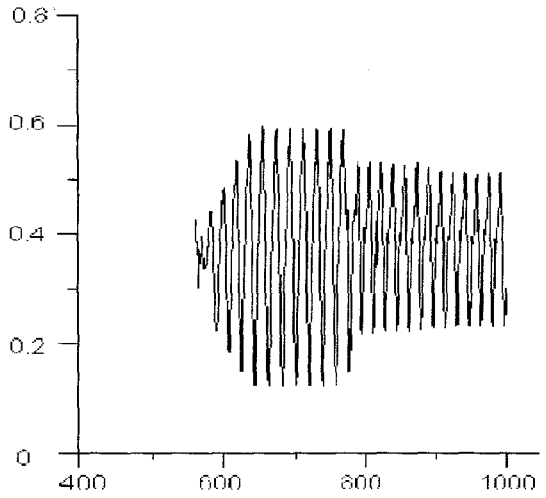


**Fig. 10**

The results of further calculations have shown that there exists a certain maximum $r_1'$ such that the amplitude again starts decreasing when this radius is exceeded (Fig. 10). The plot of $p(t)$ in Fig. 10 shows that the amplitude decreases as $r_1'$ is increased from 2.0 to 2.5 at $t = 766$. Here $r_c = 2.0$.

The study received financial support from the Russian Foundation of Basic Research (grant 99-01-00129).

## REFERENCES

1. S. B. Bazarov, G. S. Roslyakov, Yu. N. Sadkov, and M. V. Shustova, "Supersonic unrated jets and their interaction with obstacles," *Mat. Model.*, **8**, No. 6, 19–23 (1996).
2. S. B. Bazarov, G. S. Roslyakov, Yu. N. Sadkov, and M. V. Shustova, "Simulation of oscillation modes in a supersonic unrated jet flowing into a cavity," in: *Inverse Problems in Natural Science* [in Russian], MGU, Moscow (1997), pp. 181–188.
3. G. S. Roslyakov and Yu. N. Sadkov, "The effect of boundary conditions on oscillation modes in a Hartman resonator," in: *Methods of Mathematical Modeling* [in Russian], MGU, Moscow (1998), pp. 69–75.
4. A. N. Antonov, V. M. Kuptsov, and V. V. Komarov, *Pressure Pulsation in Jets and Separating Flows* [in Russian], Mashinostroenie, Moscow (1990).
5. V. N. Lyakhov, V. V. Poddubnyi, and V. V. Titarenko, *Impact of Shock Waves and Jets on Structural Elements* [in Russian], Mashinostroenie, Moscow (1989).
6. V. G. Dulov and G. A. Luk'yanov, *Gas Dynamics of Outflow Processes* [in Russian], Nauka, Novosibirsk (1984).
7. A. I. Kotov and E. A. Ugryumov, "Pulsations during the interaction of a supersonic jet with a cavity," *Vestn. LGU*, No. 1, 11–17 (1984).
8. V. N. Glaznev, V. S. Demin, and S. G. Mironov, "Experimental investigation of oscillation modes in a supersonic underexpanded jet blowing into a half-closed cylindrical cavity," in: *Gas Dynamics and Acoustics of Jet Flows* [in Russian], Sib. Otdel. Akad. Nauk SSSR, Novosibirsk (1987), pp. 85–90.
9. V. N. Uskov, V. V. Tsymbalov, and E. N. Tsymbalova, "Numerical solution of the problem of time-dependent interaction of a supersonic jet with an obstacle," *Model. Mekh.*, Novosibirsk, **1(18)**, No. 6, 151–158 (1987).

10. B. Sh. Al'bazarov, *Simulation of the Interaction of a Supersonic Jet with an Obstacle* [in Russian], Candidate Degree Thesis (Physics and Mathematics), Krasnoyarsk (1991).
11. K. W. Thompson, "Time-dependent boundary conditions for hyperbolic systems," *J. Comp. Phys.*, **68**, No. 1, 1–24 (1987).
12. Yu. N. Sadkov, "A class of third order accurate schemes for hyperbolic equations," in: *Numerical Methods in Aerodynamics* [in Russian], MGU, Moscow (1980), pp. 85–91.
13. E. A. Ugryumov, "Gas dynamics of a supersonic jet interacting with a plugged channel," in: *Gas Dynamics and Acoustics of Jet Flows* [in Russian], Sib. Otdel. Akad. Nauk SSSR, Novosibirsk (1987), pp. 66–73.
14. E. A. Ugryumov, "Gas-dynamic processes in a Hartman resonator," *Vestn. LGU*, Ser. 1, No. 4, 30–36 (1986).